International Research Journal of Engineering and Technology (IRJET) e-ISSN: 2395-0056
Volume: 11 Issue: 04 | Apr 2024 www.irjet.net p-ISSN: 2395-0072

Sustainability of Aluminum-based alloys in Chloride Ions Containing Environment

Momtazul Haque[a], O.S Bhatia[b] Lovneesh Sharma[c]

[a]*M.Tech Scholar, Department of Mechanical Engineering, Universal Institute of Engineering & Technology, Lalru*
[b]*Professor, Department of Mechanical Engineering, Universal Institute of Engineering & Technology, Lalru*
[c]*Assistant Professor, Department of Civil Engineering, Universal Institute of Engineering & Technology, Lalru*

Abstract: The fabrication of the alloys was carried out through a melting and casting method under an argon atmosphere to ensure the preservation of their inherent properties. The characterization of these samples was conducted using X-ray diffraction (XRD) and Differential Scanning Calorimetry (DSC). Vickers hardness testing apparatus was utilized to assess the mechanical properties of the alloys. The objective behind modifying the Al-12Si alloy composition was to decrease the brazing filler's melting point, a hypothesis that was later confirmed through DSC analysis. Subsequently, the alloys' resistance to corrosion was evaluated using an electrochemical potentiostat in environments containing 3.5 wt% NaCl and 0.1 M H2SO4. This allowed for a comprehensive comparison of corrosion behaviors across the various alloy compositions, focusing specifically on metrics such as corrosion current density (icorr), corrosion potential (Ecorr), and the overall rate of corrosion.

Keywords: Brazing filler, X-ray diffraction, Optical microscopy, Differential scanning calorimetry, Corrosion

Introduction:

In the fabrication of thermoelectric modules, brazing is identified as the predominant technique for joining components, leveraging a bonding agent with a melting point below those of the components being bonded. This method necessitates elevating the assembly's temperature above the bonding agent's melting point — specifically, temperatures must surpass 450°C to distinguish brazing from soldering, which employs fillers melting below this temperature [1-4].

Recent investigations have aimed at curtailing the formation of intermetallic compounds by introducing high entropy alloys as innovative brazing fillers. Such approaches have previously facilitated the effective bonding of nickel-based superalloys and solid oxide fuel cells (SOFCs) [5,6]. The high entropy concept posits that an alloy comprising multiple components in equal proportions can reduce the emergence of complex phases, favoring the development of a random solid solution where alloying elements are evenly distributed [7,8]. This notion was further illustrated by Yeh et al., who demonstrated that a high entropy value promotes the formation of a random solid solution, enhancing the alloy's homogeneity [9,10].

Particularly, the equimolar high entropy alloy Al-Si-Sn-Zn-Cu was explored as a filler material for vacuum brazing applications, especially for joining Al-based superalloys. Remarkably, the liquidus temperature of this alloy stands at 1346 degrees Celsius, significantly exceeding the solution treatment temperature range for Mar-M 247, typically between 1080 and 1170 degrees Celsius [11]. The initiative to modify the Al-12Si alloy aimed at reducing the brazing filler's melting point has been substantiated through DSC analysis. Furthermore, the corrosion resistance of the developed alloys was assessed in a 3.5 wt% NaCl solution, enabling the comparison of corrosion parameters across the various alloys produced.

Figure 1 Various Classes of HEAs as Brazing Filler

Material and Methods:

2.1. Materials:

For this study, the initial step involved utilizing the received powders of aluminum, copper, cobalt, molybdenum, silicon, tin, and zinc to prepare the alloy samples. These raw materials were carefully measured out in precise proportions to match the targeted compositions for the alloy synthesis. (Table 1).

Table 1 Composition of alloys (wt.%)

Compositions	Co	Mo	Si	Sn	Zn	Cu	Al
C0	0.5	0.5	12	0	0	0	Balance
C1	0.5	0.5	12	0.75	0.75	2	Balance
C2	0.5	0.5	12	0.75	0.75	4	Balance
C3	0.5	0.5	12	0.75	0.75	6	Balance
C4	0.5	0.5	12	0.75	0.75	10	Balance

First and foremost, the powders were taken and combined into the mortar in accordance with the compositions. Then, using a 15 mm diameter die mounted in uni-axial compaction machinery, the powders were compacted to produce the final product. The pellets were made in this manner and were of five distinct compositions. In the next step, the pellets were inserted into the copper mold, and the requisite vacuum level was obtained, after which inert argon gas was purged from the copper mold. Finally, the pellets were melted five times with a spark, the strength of which may be controlled by varying the current flow rate in the circuit. By impacting electrons with a large amount of kinetic energy, the temperature of the material will rise very quickly very quickly.

2.2. Methods

Extensive phase investigation of aluminum-based alloy samples was carried out using XRD, which operates on the basis of Bragg's Law. Equipment using Cu radiation was used to conduct XRD experiments on a variety of various compositions. The samples were put on a silicon wafer and agglomerated with acetone after being soaked for many hours. The analysis was carried out in the 2o range of 20o-90o using a 10 second scan and a 2º step size of 0.04 º in the 2º range of 20º-90º. All XRD peaks were fitted using peak fitting to get the peak locations and full width at half maxima, which were then computed. The XRD data was also used to determine the lattice parameters of the crystal. Differential Scanning is a kind of scanning in which two or more images are compared side by side. For thermal examination of materials in which phase transitions such as melting, glass transitions, or exothermic decompositions are investigated, the calorimetry method is utilized. Both the reference sample and the sample on which thermal analysis is to be performed are necessary for this experiment to be completed. The reference sample should have a well-defined heat capacity across the temperature range that will be scanned in order to be useful.

For the optical microscopy, the sample were polished with SiC abrasive papers with grit size 220, 400, 600, 800, and 1000 in a series, after which polishing was done using velvet cloth having alumina suspension diluted with water on a double disk polishing machine. For the hardness of the samples, the samples was kept under the indenter of hardness testing apparatus, and 3kgf load will be applied for 15 seconds of dwell time. After using load and keeping that load for the decided dwell time, the indenter will be released. For the purpose of ensuring repeatability in the corrosion tests, the tests were carried out three times on each sample, repeatedly. The experiment began with the plot of the OCP (Open circuit potential), and after a stable condition had been attained, the polarization curves were constructed using the data from the plot. The values of e_{corr} and i_{corr} were found after T_{afel} fitting.

3. Results and Discussions

3.1. X-Ray Diffraction of Al-based alloys

We performed XRD analysis on each and every one of the aluminum-based alloys we tested in order to determine which phases were present in the alloys. Figure 2 shows crystalline peaks of two separate phases of aluminum and silicon that may be distinguished. According to certain theories, the strength of the Si peak has been weakening as a consequence of the creation of supersaturated Si solutions in the Al, as well as the rapid cooling rates that were seen throughout the melting and casting processes. For each XRD pattern illustrated below, the values of (h k l) planes, d spacing for the corresponding element, and angle 2 theta are computed and tabulated. Because the alloying elements Co, Mo, Sn, Zn, and Cu were completely dissolved and a solid solution produced, it is not feasible to observe peaks for these elements in the resulting analysis in figure 2 of C1. When comparing the other alloying elements, including alloys, to the single Si-containing alloy, the intensity of the Al and Si peaks in the other alloying elements, including alloys, is substantially decreased in comparison to the single Si-containing alloy (C_0).

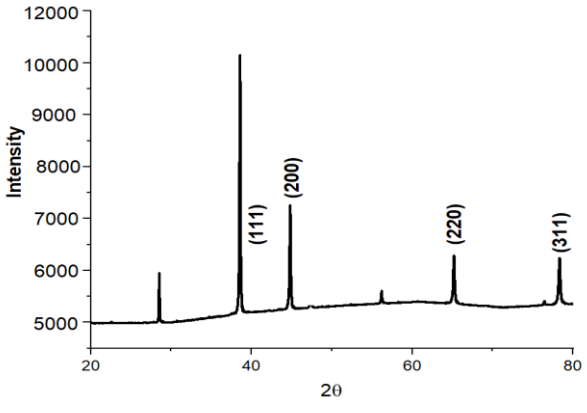

Figure 2. XRD pattern of C0 alloy

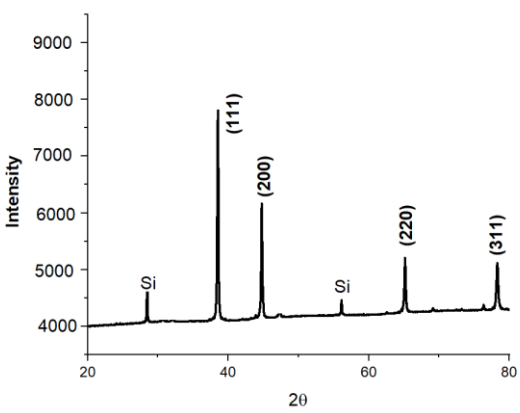

Figure3. XRD pattern of C1 sample

3.2. Prominent XRD Analysis

This migration of the most prominent XRD peak of alloys from its original location to its left side indicates that the lattice expansion of Al atoms has happened as a consequence of solid solution formation with alloying elements (Co, Mo, Cu, Sn, Zn, Si). As the concentration of Cu in the solution rose, the lattice structure continued to grow as seen in figure 4.

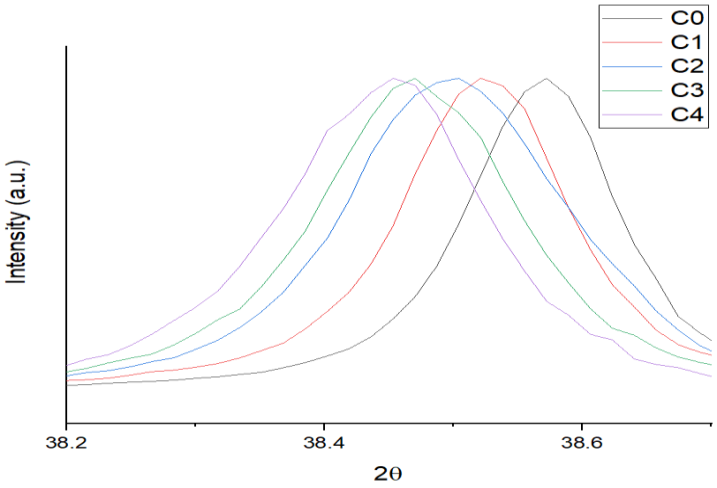

Figure 4. The Prominent XRD peak shift of Al-based alloys

3.3. DSC and Optical Microscopy

The DSC study was carried out on all of the Al-based alloys that are presently being synthesized. All alloys were submitted to DSC testing up to 700 degrees Celsius. In general, the melting point of Al-based alloys declined as the amount of Cu in the alloy rose, as seen in Figure5. 570ºC was reached by the C0 alloy before the AlSi eutectic reaction took place, indicating that the first phase transition had been achieved. 590.6 degrees Celsius was revealed to be the melting point of C0 alloy, according to research. The melting point of the metal decreased when alloying was introduced. Furthermore, when the Cu concentration grew, the melting point decreased. Because filler materials should have the lowest melting point possible, it means that the Cu addition makes the alloy more suitable for use as a filler. The optical micrographs of all the alloys are shown in Figure 6.

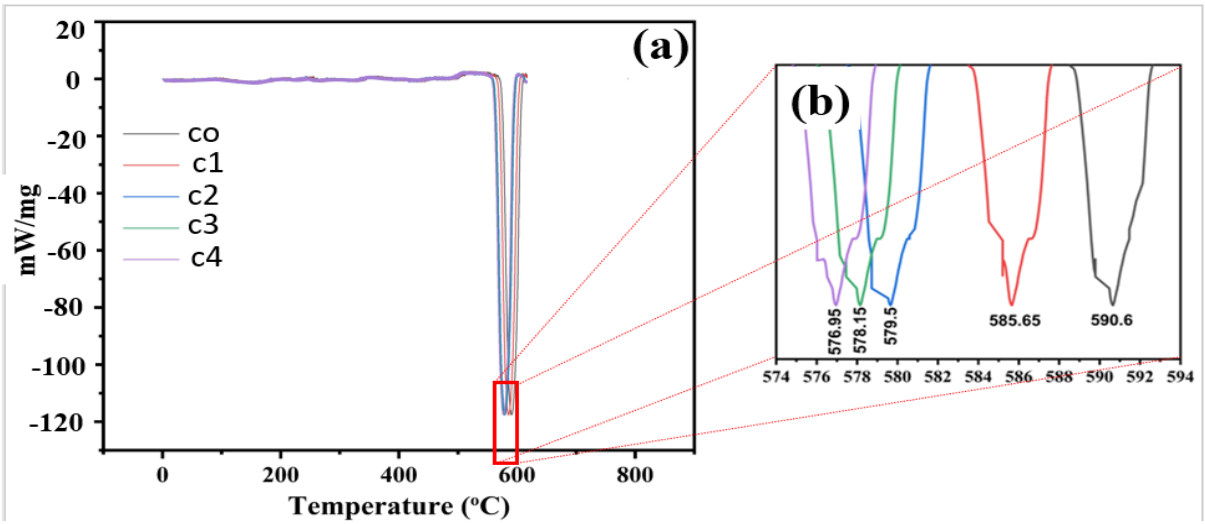

Figure 5.DSC of Al-based alloys

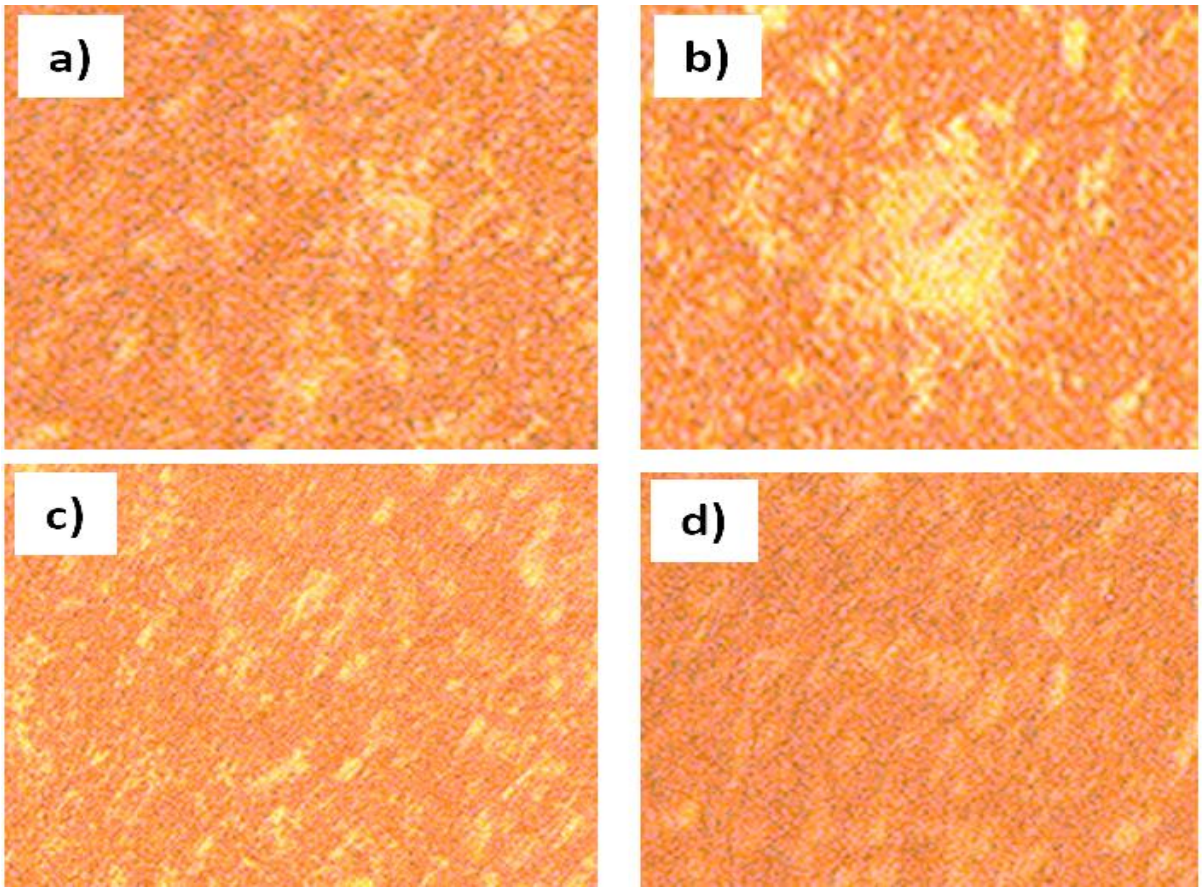

Figure 6 Optical micrographs of a) C1, b) C2, c) C3, and d) C4

3.4. Electrochemical analysis of Al-based alloys in 3.5% NaCl solution

After the polished samples of aluminum-based alloys were linked with copper wire and subsequently mounted in epoxy resin, just one surface with a surface area of one centimeter square (cm^2) was subjected to corrosive conditions. The sample was used as the working electrode, and it was placed in a three-electrode glass cell with a counter electrode (platinum mesh) and a reference electrode to conduct the experiment (SCE). Each experiment started with an hour of ocp (open circuit potential) to allow the sample to stabilize in the corrosive liquid before continuing. The potentiodynamic polarizaton curve was then generated by scanning the electrodes at a rate of 0.5 mV/s. Using the tafel fit, it was possible to determine the electrochemical parameters of the sample, such as the corrosion potential (Ecorr) and the corrosion current density (icorr). Because the corrosion rate (CR) is closely related to the corrosion current density (icorr), the value of icorr was used to compute the corrosion rate (CR). In order to compute CR, it was required to take into account two more factors: density and equivalent weight. Figure 7 shows the potentiodynamic polarization curves of all of the alloys, which were created in a 3.5 weight percent NaCl solution in order to highlight the influence of Cu on corrosion behavior. The drop in corrosion potential implies a decrease in the susceptibility to corrode, and the decrease in current density indicates a decrease in the rate of corrosion.

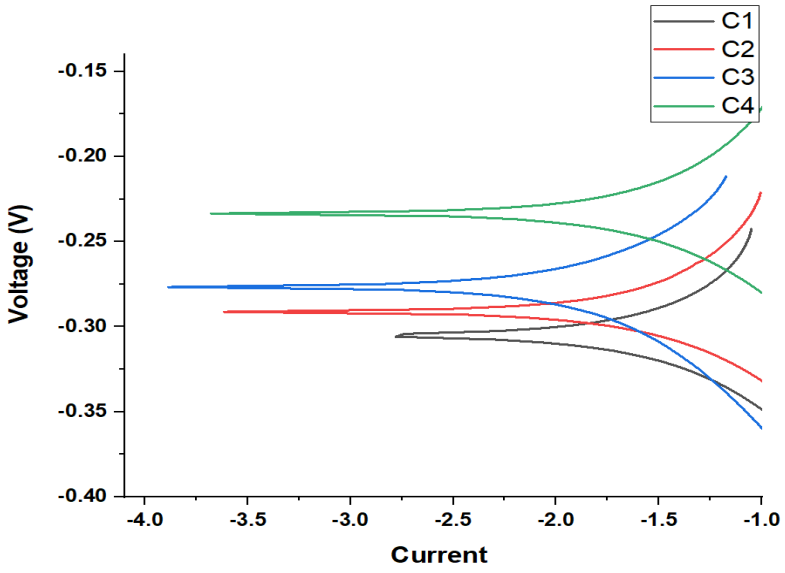

Figure 7. Potentiodynamic polarization curves of samples in 3.5 wt% NaCl aqueous solution

Conclusion: The fabrication of aluminum-based alloys was achieved through a process of melting and casting. Introduction of various alloying elements, and notably copper, led to a reduction in the alloys' melting points. This reduction was particularly marked up to a specific level of copper addition. As the copper concentration was elevated, there was a noticeable increase in the alloys' densities, although these measured densities were marginally below the calculated theoretical values, likely due to the presence of porosity within the materials. Enhancements in the hardness of the alloys were observed in correlation with rising copper percentages. Among the compositions evaluated, the C3 alloy exhibited outstanding corrosion resistance in a saline solution of 3.5% NaCl, outperforming the other alloys subjected to the same conditions.

Conflict of Interest: Authors declare no conflict of interest.

References:

1. T. Onzawa, A. Suzumura, and M. Ko, “Brazing of titanium using low-melting-point Ti-based filler metals,” Welding Journal, vol. 462, 1990.

2. A. E. Shapiro and Y. A. Flom, “Brazing of titanium at temperatures below 800°C: review and prospective applications,” DVS Berichte, vol. 243, p. 254, 2007.

3. B.S. Murty, J.W. Yeh,.; S. Ranganathan,”High. Entropy Alloys, 1st ed.”; Butterworth-Heinemann: London, UK, 2014.

4. M. Way, J. Willingham, R. Goodall, Brazing filler metals, Int. Mater. Rev. 0 (2019) 1–29. https://doi.org/10.1080/09506608.2019.1613311

5. Tillmann W, Wojarski L, Manka M et al. (2018) Eutectic high entropy alloys—a novel class of materials for brazing applications, Proceedings from the International Brazing & Soldering Conference, 15th to 18th April 2018, New Orleans, pp 142–148

6. Hardwick L, Rodgers P, Pickering EJ et al. (2019) Development of novel nickel-based brazing alloys, utilising alternative melting point depressants and high entropy alloy concepts, Proceedings from Brazing, high temperature brazing and diffusion bonding, 12th International Conference, 21st to 23rd May 2019, Aachen, pp 7–17

7. Tillmann W, Wojarski L, Ulitzka T et al. (2019) Brazing of high temperature materials using melting range optimized filler metals based, Proceedings from Brazing, high temperature brazing and diffusion bonding, 12th International Conference, 21st to 23rd May 2019, Aachen, pp 1–6

8. Cantor B, Chang ITH, Knight P et al (2004) Microstructural development in equiatomic multicomponent alloys. Mater Sci Eng A 375-377:213–218. https://doi.org/10.1016/j.msea.2003.10.257

9. Zhang LX, Shi JM, Li HW et al (2016) Interfacial microstructure and mechanical properties of ZrB 2 SiC C ceramic and GH99 superalloy joints brazed with a Ti-modified FeCoNiCrCu high-entropy alloy. Mater Des 97:230–238. https://doi.org/10.1016/j.matdes. 2016.02.055

10. Yeh J-W (2013) Alloy design strategies and future trends in highentropy alloys. JOM 65(12):1759–1771. https://doi.org/10.1007/s11837-013-0761-6

11. Baldan R, da Rocha RLP, Tomasiello RB et al (2013) Solutioning and aging of MAR-M247 nickel-based superalloy. J Mater Eng Perform 22(9):2574–2579.